Modelling flaming combustion in glass fibre-reinforced composite laminates

A Thermal Model For Spontaneous Combustion Of Fibre-Reinforced Composite Laminates

E.D. M[c]Carthy[1], B. Kandola[1]*, E. Kandare[1,3], P. Myler[1], G. Edwards[1], Yong Jifeng[3], Yong C. Wang[3]

1. Institute For Materials Research and Innovation, University of Bolton, BL3 5AB, UK

2. Dept. Of Aerospace Engineering, RMIT University, PO Box 2476V, Melbourne, Australia

3. Mechanical, Aerospace and Civil Engineering, The University of Manchester, M60 1QT, UK

ABSTRACT

A heat transfer model based on the well-known Henderson's equation has been enhanced to allow ignition and combustion phenomena of fibre-reinforced structural composite materials to be predicted from first principles using known physical and thermodynamic data for their constituents. This enhancement has consisted of two principal components; 1) a mathematical mechanism for recognition of the accurate time to and temperature of ignition, and 2) an incorporation of the heat of combustion generated during the exposure time of interest. This has allowed a model of good qualitative character to be achieved, which generally replicates mass and temperature data obtained by cone calorimetric experiments for two types of composite laminates, a control E-glass / epoxy composite and a fire retarded laminate, where the resin contains fire retardant chemicals as additives. There however remains the challenge of improving the quantitative fit of the model by obtaining more accurate volatiles diffusivity / permeability parameters, as well as a fully representative quantitative understanding of the volatiles released during decomposition of the two different composite materials. It is anticipated that both these measures will result in a model of more accurate quantitative fidelity to cone calorimetry data, which may ultimately be used as a partial substitute for experiment in the early stages of composite formulation and fire testing.

***Keywords**: composites, epoxy resins, flammability, fire retardants, modelling, spontaneous combustion, heat transfer model*

1 Introduction

The fire-resistance and mechanical resilience of glass fibre-reinforced epoxy laminate structures to thermal radiation is of crucial importance to their use and specifications in key aerospace, marine and automotive applications. In particular, the ability of these laminates to retain structural integrity and mechanical strength for the longest possible time after ignition is a key objective. In cases where it is not possible to prevent ignition completely or even delay it significantly using fire retardant chemicals, it is then necessary to assess the time at which a composite will lose its structural integrity, the rate with which this will occur, and most importantly, the severity of this strength loss. Normally, in order to do this, it is necessary to perform experiments which reproduce as closely as possible the worst hazards to which the composite may be exposed and thereby derive data which allows material designers and engineers to specify materials and designs with maximum confidence. However, it is becoming increasingly desirable to model the combustion process numerically using mathematical simulation so as to screen new resins and additives early in the design process, well in advance of experiments and industrial scale-up and assess as accurately as possible their inherent resistance to heat exposure and fire damage. Such theoretical models should also help engineers to better understand and control the thermal and chemical processes underlying heat damage and combustion, providing an early opportunity to reformulate where inherent weaknesses are identified. In the longer term, highly accurate predictive computer models of the combustion process, which have been closely validated by experimental data, offer the potential to partially or even wholly replace experimental testing as the principal means of validating the fire resilience of structural composites.

The mathematical modelling of combustion in fibre-reinforced composite laminates is a complex task requiring consideration of heat transfer, the chemistry and kinetics of decomposition and combustion, the mass transport of volatiles through melts and chars as well as the effect of temperature on mass loss the laminate immediately before, during and after ignition. This information can give insight of

accompanying mechanical property retention of these laminates. A number of researchers have tackled this challenge in numerous works. The Henderson model [1] consisting of 3 coupled partial differential equations describing heat transfer, mass transfer and the chemical kinetics has remained the starting point for most researchers since. More recently Gibson & Mouritz [2], Drysdale [3,4], Lyon [5,6], Staggs [7-11], and Galgano et. al. [12] have provided refinements of the Henderson model which examine different aspects of the combustion problem using different modelling approaches. However in many of these models there is no mechanism to predict sharp discontinuities or step-changes in temperature which occur during a sudden ignition event, particularly at or near laminate surfaces, (e.g. Figure 2). Instead current models present surface temperature predictions which are continuous mathematical curves, incapable of modeling discrete rapid, surface events such as ignition. The present model has been designed to include such a predictive capability, by treating the ignition event as an added source of heat, which is activated under certain thermodynamic conditions.

This work presents further refinement of our recently developed heat transfer model, Kandare et. al., [13], based on Henderson's equation, which predicts the through-thickness temperatures of the laminates exposed to radiant heat, but only prior to ignition of the laminate. The refinement allows measurement of time and temperature of ignition, and through-thickness temperature profiles of the burning laminates. The development of the model and its validation with experimental results is discussed in chronological order in the following sections.

2 Materials and Heat/Fire Exposure Scenario

For validation of models discussed in subsequent sections, eight ply glass – fibre reinforced composite laminates were fabricated via a wet lay-up method using a low-viscosity and low temperature-curing base epoxy resin containing 1,4-butanediol diglycidylether, (Araldite LY5052) and a hardener based on modified cycloaliphatic amines (HY5052) (Huntsman, Inc.); woven roving E glass (300 g/m^2) (Glasplies,

UK). The composite fabrication details are given elsewhere [13]. Two types of composite laminates were prepared; a control (EP) and a fire-retarded sample (EP20) containing 20% w/w fire retardant additives in the resin. The fire retardant additives included 10% (w/w) Visil®, a cellulosic fibre containing polysilicic acid, chopped fibres (from an initial length of 40 mm, 3.5 dtex and diameter 17 μm) (Sateri Fibres, Finland) and 10% (w/w) of intumescent, (Antiblaze® NH, Rhodia Specialities UK). The fibre volume fractions were calculated to be 32 and 28% for EP and EP20, respectively. The thickness of both composite laminates was 3 ± 0.2 mm and master laminates of 300 mm^2 were laid up. From these master laminates, standard cone plaques of 100 x 100 mm were cut. K-type thermocouples were inserted at the top, fourth and eighth ply layers respectively within each of these test plaques during the wet lay-up process, to measure surface, middle and base temperatures progressively with exposure time. Data was recorded every second during heat exposure to a maximum of 600 s.

Heat exposures of the laminates were performed using a FTT (Fire Testing Technology, UK) cone calorimeter in the horizontal mode with an ignition source at an applied heat flux of 50 kW/m^2. Laminates in each case were mounted at 25 mm distance from the base plate of the cone heater. Both the unheated base and sides of each laminate were insulated using a ceramic wool and aluminium foil, to ensure that the boundary conditions of the model, (i.e. no heat transfer across the base and sides of the slab), were reproduced as far as practically possible. Multiple exposures of both laminates were performed, with good reproducibility of temperature profiles.

The physical properties determined by experiment for these two composite samples are reported in Table 1, with details given elsewhere, [14]. These consist of the Arrhenius parameters of the decomposition reaction represented as a first-order, single-step decay of the primary resin, as well as the heat of decomposition for this reaction as determined from DSC measurements.

3. Heat Transfer Model without Ignition or Combustion; Model A

As discussed in Section 2, the fundamental problem description is that for a structural laminate exposed to a steady-state radiant heat flux on one side, while fully insulated on the opposite (bottom) surface. This is a case of asymmetric heat exposure and a schematic diagram of the laminate is shown in Figure 1. In the figure, the principal heat transfer processes, described as flows of heat into, through and out of the laminate are represented. An external steady-state heat flux radiates upon the top surface of the laminate, part of which is absorbed into the bulk of the material, and part of which is either re-radiated back into the headspace or is convected back into the headspace fluid, (usually air). The proportion of heat which is actually absorbed is principally a function of the radiative emissivity of the surface, the convective heat transfer coefficient from the surface to the headspace fluid, and the conductivity of the bulk material itself.

The surface temperature of the laminate, T_s is governed by the relative flows of heat of each of these mechanisms; radiation, convection and conduction through the bulk, and would assume an equilibrium value at a steady-state external heat flux, if there were no chemical reactions within the bulk laminate material. However, such a condition of physical heat transfer without chemical reaction is not the case where thermoset resins (or polymeric materials in general) are concerned. In the case of epoxy resins (and other polymers), decomposition occurs at a critical temperature, whereby the resin progressively degrades to form a mixture of volatile products and solid residue product known as primary char. The primary char further degrades to form other volatile products and a carbonaceous char. The volatile products can be combustible, but the carbonaceous char is incombustible.

3.1 Theory and model

3.1.1 Heat Transfer

The fundamental equation describing the heat transfer in a solid plaque of a material is the Henderson equation given by (1), [1]

$$\rho c_p \frac{\partial T}{\partial t} = \frac{\partial}{\partial x}\left(k \frac{\partial T}{\partial x} \right) - \frac{\partial}{\partial x}\left(\dot{m}_{vol} h_{vol} \right) - \frac{\partial \rho}{\partial t}\left(Q_{decomp} + h_{char} - h_{vol} \right) \quad (1)$$

In Equation (1) ρ is the density of the composite solid, c_p is its specific heat capacity, T is temperature, m_{vol} is the mass flow rate of volatiles generated by decomposition, h_{vol} is the corresponding enthalpy of the volatile mixture, Q_{decomp} is the heat of the decomposition reaction, and h_{char} is the enthalpy of the char produced. In the expression, the term on the left hand side represents the rate of change of the heat stored within the laminate, which is balanced on the right hand side by terms for conduction within the laminate, loss of enthalpy through volatile escape, and a term balancing the heat of decomposition with the changing balance between volatile and char enthalpy which accompanies the reaction. The partial differential equation (1) is supplemented by boundary conditions.

For the surface exposed to the radiating source the boundary condition contains a radiation term - the Stefan Boltzmann law and a convection term. The heat balance equation at the surface is:

$$\dot{Q}_{net} = \dot{Q}_{ext} - \varepsilon\sigma\left(T_s^4 - T_h^4 \right) - h_{conv}\left(T_s - T_h \right) \quad (2)$$

For the insulated, (bottom), surface, the boundary condition is:

$$\dot{Q}_{net} = \frac{\partial T}{\partial x} = 0 \quad (3)$$

The flow of heat through the laminate is modeled by the differential equation , (Eqn. 4)

$$\frac{\Delta Q_i}{\Delta t} = \frac{x_i \rho c_{p,c} \Delta T_i}{\Delta t} = k\left(\frac{\left(T_{i-1} - T_i \right)}{\left(x_i + x_{i-1} \right)/2} - \frac{\left(T_i - T_{i+1} \right)}{\left(x_i + x_{i+1} \right)/2} + Q_{decomp,i} + Q_{comb,i} \right) \quad (4)$$

This may be expressed in a discretised form using the finite-difference representation of spatial derivatives, (5):

$$\frac{dQ_i}{dt} = \frac{\partial\left(x_i \rho c_{p,c} T_i\right)}{\partial t} = k\left(\frac{\partial T}{\partial x_1} - \frac{\partial T}{\partial x_2}\right) + Q_{decomp,i} + Q_{comb,i} \quad (5)$$

Furthermore, two variations of Eqn. 5 are written for transmission near the surface, (i = 1 or s), and base, (i = n), of the laminate; (6) and (7) respectively, both of which are adjusted to reflect the boundary conditions at the surface and base of the laminate respectively as follows:

$$\frac{\Delta Q_1}{\Delta t} = \frac{x_1 \rho c_{p,c} \Delta T_1}{\Delta t} = \left(Q_{net} - \frac{k\left(T_1 - T_2\right)}{\left(x_1 + x_2\right)/2}\right) + Q_{decomp,i} + Q_{comb,i} \quad (6)$$

$$\frac{\Delta Q_n}{\Delta t} = \frac{x_n \rho c_{p,c} \Delta T_n}{\Delta t} = \left(\frac{k\left(T_{n-1} - T_n\right)}{\left(x_n + x_{n-1}\right)/2}\right) + Q_{decomp,i} + Q_{comb,i} \quad (7)$$

Since decomposition and combustion processes are also active within the laminate, it is necessary to include extra terms for the heats of decomposition and combustion The conditions under which the term for heat of combustion, $Q_{comb,i}$ is employed are discussed in Section 6.

This complete set of equations can be solved for determination of temperature profile through a laminate using known values of heat capacity, density, thermal conductivity and the heats of decomposition and combustion of the resin and decomposition products respectively.

3.1.2 Decomposition Kinetics

There is a diverse literature on the subject of polymeric decomposition and associated kinetics [6]. Study and modelling of polymer decomposition usually involves thermogravimetric (mass loss) studies under controlled constant heating rate conditions. Models can range from relatively straightforward ones assuming a single-step and based on first-order kinetics [11] to more complex models involving multi-component degradation with different reactions occurring both in series and parallel, [15, 16]. In the present model for a cured epoxy resin *either with or without additives*, a simple single-step degradation scheme is used, which is predicated on the assumption that w units of the resin degrade to form products

with a selectivity of $s_{char} = w_{char}/w$ towards char, (char yield), and $s_{vol} = w_{vol}/w$ towards volatiles. This is done to simplify the development of the model and speed up the validation of a "proof-of-concept" in a simulation which involves many other interacting parameters, the effect of each of which must be separately determined. Once this simplified model is validated it is intended to insert more sophisticated calculations for both the kinetics of degradation, and the proper calculation of changing, weighted physical properties for the solid composite as decomposition and combustion progresses. Thus the degradation of the resin, with or without included additives, within a 50:50 w/w E-glass-epoxy composite using a single-step first order degradation reaction described by equations (8 - 9) was simulated. Here, equation (8) describes the temperature dependence of the decomposition reaction rate constant k_{decomp}, (9) is the first-order mass decay law applied to the degradation, and (10) is an integrated form of (9), for a known initial concentration of resin, $m_{resin,0}(t)$.

$$k_{decomp}(T) = A\exp(-E_a/RT) \tag{8}$$

$$\frac{dm_{resin}}{dt} = -k_{decomp}.m_{resin} \tag{9}$$

$$m_{resin}(t) = m_{resin,0}(t)\exp(-k_{decomp}.t) \tag{10}$$

In the present model, which is expressed in terms of resin, char and volatile fractions, expression (10) has been replaced by a linear corrective model for the instantaneous fraction of each component as a function of time i.e. (11-13). Such an expression is best suited to a finite difference model which updates in time increments. The expression of component masses as fractions also allows the instantaneous thickness for each layer, i, within the laminate, to be more efficiently calculated.

$$f_{resin,i,t+1} = f_{resin,i,t.}(1-k_{decomp,i}t) \tag{11}$$

$$f_{char,i,t+1} = f_{char,i,t} + s_{char}.k_{decomp,i}.f_{resin,i,t}.t \tag{12}$$

$$f_{vol,i,t+1} = f_{char,i,t} + s_{volatiles}.k_{decomp,i}.f_{resin,i,t}.t \tag{13}$$

3.1.3 Thickness of Laminate during Decomposition and Combustion

The change in the thickness x_i of the i^{th} layer as a function of the instantaneous solid concentrations of resin and char in that layer $f_{resin,i,t}$ and $f_{char,i,t}$. is calculated by (14).

$$x_{i,decomp} = x_{i,0}\left(f_{resin,i,t} + f_{char,i,t}\right) / f_{solid,i,0} \quad (14)$$

In this expression $x_{i,0}$ represents the original thickness of each layer i of n layers prior to decomposition. The variables $f_{resin,i,t}$ and $f_{char,i,t}$ represent the fractions of resin and char and $f_{solid,i,t}$, the original solid fraction of the laminate, which is initially unity on a void-free basis. The separate effect of solid expansion with temperature is neglected within the present model.

3.2 Operation and Structure Of The Model

3.2.1 Operation of Model

The solution of the overall predictive heat transfer model consists of solving the principal finite difference equations (2) and (5-7) described above. These are supplemented by auxiliary equations (8) and (10), which describe decomposition, (11 – 13), which calculated the instantaneous fractions of resin, char and volatiles in each layer i. Eqn. (14) describes the receding thickness of the laminate. This system is solved by use an iterative calculation process which allows initial values for variables to be progressively corrected, as the entire simulation converges towards the correct solution.

3.3 Results and Validation of Model A

The model was applied to simulate the degradation of two composite laminates, glass/epoxy control composite EP and flame retarded composites EP20, where the resin contains flame retardant additives. These two samples were chosen to test the validity and sensitivity of the model as in these two samples the resin matrix has different physical and kinetic parameters. EP and EP20 were exposed to one-sided external heat flux of 50 kW/m^2 in a cone calorimeter and the resulting through-thickness temperature

profile and mass loss results are provided for the EP composite in Figures 2(a) and 3(a), and for the EP20 composite in Figures 4(a) and 5(a).

In the case of EP, (Fig. 2(a)), it can be seen that Model A overestimates the surface temperature to qualitative accuracy until approximately 74s, where ignition occurs and it does not recognise the actual ignition event and hence, underestimates the data between 74 and 177 s. Since the model is only a heat transfer one, the latter part is not unexpected. However, the discrepancy between the simulated and experimental data for middle and the bottom surface temperatures is less. The simulated surface and bottom temperatures converge at about 177 s whereas experimental values converge much later at 215 s. When applied to EP20 data, (Fig. 4(a)), this model shows a better fit for surface and middle temperatures before ignition, however, the simulated surface and bottom temperature curves converge at approximately 255 s, as opposed to the corresponding actual temperatures which did not converge within the 400 s of the test. The discrepancy observed for the bottom temperature could be due to the reason that either the conductivity of the sample in the model is consistently overestimated or its specific heat capacity is underestimated or both.

The corresponding mass loss curves for the EP 50 kW m^{-2} exposures are shown in Figures 3(a) and 5(a). In Figure 3(a), the non-ignition model systematically underestimates the real rate of mass loss, which corresponds to the ignition point as illustrated by Figure 3(a). This is surprising when it is considered that ignition, and the additional heat it supplies to the laminate is not modelled. Indeed, it might be expected that the model would underestimate the extent of mass loss in this circumstance. In Figure 5(a), the actual (experimental) mass loss data for the EP20 composite specimen is reported and compared with the output of the non-ignition simulation. Again as with the EP mass loss model, it is clear that Model A is insufficient to represent the actual mass loss data with the model overestimating the rate of mass loss in the time domain $8 < t < 74$ s, after which it begins to overestimate the rate of mass loss reaching a limiting finite value of approximately 60% residual mass at 240 s. Since the resin mixture contains 20 wt-% of

incombustible additives, this result implies that there is practically no formation of char predicted by the model. The mass loss data, however, indicates a much longer and more gradual mass loss process with a higher residual mass threshold of 63%, indicating a residual char of approximately 3%. It is not entirely surprising that this non-ignition model is incapable of modelling either temperature or mass loss after 74 s, due to the onset of fully-developed combustion, but it is of concern that Model A, the non-ignition model, is not adequately predicting either bottom or surface temperature in the heating phase of the exposure prior to ignition and combustion.

Thus, it is necessary to examine ways in which to improve this non-ignition model, (Model A), before any attempt can be made to add a predictive capability for ignition. Two steps are ~~immediately suggested undertaken~~; the incorporation of code to make physical properties responsive to changes in temperature as previously done by Galgano et. al. [12], among others, and the incorporation of a module to accurately represent the mass transfer of volatiles out of the laminate and into the headspace. These two are discussed below as Models B and C, respectively.

4. Model B: Temperature-Dependent Physical Property Data

Model A, does not model the variability of composite thermal properties in advance of ignition. Thus it is necessary to obtain a) accurate values for the physical properties of the laminate which can be calculated as weighted estimates of the constituent components and b) an accurate expression for the temperature dependency of each of these component properties and the weighted composite values.

4.1. Physical Property Measurement

4.1.1 Density of the composite laminate

The effective densities of the control EP and the fire-retarded EP20 composite laminates were determined as a function of increasing temperature, discussed in details in our previous publication [14], the results are shown here in Figure 6(a). Composite density was determined by the measured weight and volumes

of samples in respect of each solid state, virgin polymer and charred residue. This was achieved using a formula for mixture density given by Eqns. (15) and (16) and substituting experimental values for the unburnt glass fibre- resin laminate and heat damaged fibre- char residue respectively.

$$\rho(T) = \alpha(T)\rho_{fibre-char} + (1-\alpha(T))\rho_{resin-char} \quad (15)$$

$$\alpha_i = (100 - f_{char,i})/(100 - f_{final,char}) \quad (16)$$

4.1.2. Specific Heat Capacity Of The Composite Laminate

Specific heat capacity was determined using differential scanning calorimetry of both the pure EP resin, and resin mixed with fire-retardant additives, EP20, over the range of temperature of interest, (to 627 °C = 900 K), as reproduced in Figure 6(b). The specific heat capacity of glass fibre was allocated a value of 840 J kg^{-1} K^{-1} based on a literature value sourced by Kandare et. al., [14]. The heat of decomposition was also derived by measurement of the area under the appropriate peak in the same DSC scan.

4.1.3 Thermal Conductivity of the Composite Laminate

The thermal conductivities of the composites as a function of temperature was determined by Lee's Disk Method, [16], for both the virgin fibre-resin composites and the residual, cooled fibre- char solids, resulting in curves as reproduced in Figure 6(c). For the case of estimating thermal conductivities of composite materials it is conventional to use a reciprocal weighting law to calculate the value as opposed to the additive equation used in the case for effective composite density in Section 4.1.1. This reciprocal law is given by Eqn. (17) in a manner similar to that used by Galgano et. al., [12], where the α(T) is the conversion towards char, Eqn. (16).

$$\frac{1}{k(T)} = \frac{\alpha(T)}{k_{fibre-char}} + \frac{1-\alpha(T)}{k_{resin-char}} \quad (17)$$

4.1.4 Density and Specific Heat of Volatiles

The density of the volatiles mixture generated by laminate decomposition is a function of temperature, because of the phenomenon of thermal expansion. In the present model, we are using methane as the sole representative species for what in reality is a mixture of volatile species such as lower alkanes and phenolic moieties produced by the degradation of epoxy resin, [18], pending more characterisation.

The expansion behaviour of methane may be approximated by an equation of state such as (18), [20], which expresses the instantaneous specific volume of a volatiles, v / [mol m^{-3}], as a function of temperature, T / [K], pressure, P / [Pa], the real gas constant, R / [J mol^{-1} K^{-1}], and the compressibility of the volatile mixture, z, which expresses its departure from ideal behaviour.

$$v_{CH_4} = \frac{zRT}{P} \tag{18}$$

This equation is plotted in Figure 7(a). Specific volume can be converted to a mass density value in kg m^{-3} using the known molecular weight of the volatile, (Figure 7b). The specific heat capacity of methane is not constant but is a direct and almost linear function of temperature. The curve corresponding to this linear dependence is calculated using an atom contribution method as related by Perry et. al., [22], and is reproduced in Figure 8.

$$c_{p_{CH_4}} = A_1 + A_2 C + A_3 H \tag{19}$$

4.2 Results and Validation of Model B

The results of the modified heat transfer model, Model B are shown in Figures 2(b), 3(b), 4(b) and 5(b). Although there was no effect of incorporating temperature dependence of the laminate physical properties on the simulated temperature values up to about 160 s in both EP and EP20 samples (see Figure 2(b) and 4(b), a radical change in the shape of the predicted temperature curves is observed after 160 s.

Instead of the convergence of surface and bottom temperature which occurs in Figure 2(a) for sample EP for the constant-properties model at approximately 177 s, there is instead a more gradual convergence of the temperature to a value of ~ 610°C at 300 s, which is a clear improvement in the model, although the final temperature is somewhat overestimated relative to the data. The corresponding mass curve in Figure 4(b) is also different to that produced in Figure 3(a) by the constant properties model, (Model A). It is now much qualitatively much closer to the data, though still underestimating the true extent of mass loss. Similarly for EP20 in Figure 5(b), the mass loss is similarly overestimated. This is perhaps not surprising when it is considered that since Model B does not yet model ignition or combustion phenomena, it is more likely to underestimate true mass loss than overestimate it. Overall there is no significant effect of incorporating the additional assumptions of Model B

5 Model C: Heat Transfer Model with Mass Transport Of Volatiles

A calculation for the diffusion of volatiles through a polymeric laminate is necessary in any model of composite degradation and flaming combustion behavior as follows.

5.1 Theory of Volatile Mass Transfer through Thermoset Materials

The equation for diffusion of volatiles is given by Lautenberger et. al., [26] according to which:

$$\dot{m}_{vol}(x,t) = -\beta_T \rho (1 - f_{char}) \frac{\partial T}{\partial x} \tag{20}$$

where, the instantaneous mass flux of volatile mixture at time, t and position x within the laminate, is the product of a thermal volatile diffusivity coefficient, β_T, [$m^2\ s^{-1}\ K^{-1}$], the density of the polymer melt, ρ, the proportion of volatiles formed by decomposition within the laminate, (1-f_{char}), and the temperature gradient through the laminate. Physically, the basis of the equation is that the velocity of volatiles is proportional to the negative viscosity gradient within the laminate, which itself is inversely proportional to the temperature gradient, hence the negative sign on the right hand side of the equation, [26]. The

result is that when this equation is employed in a flaming combustion model, an upward flow of volatiles through the laminate is simulated, consistent with the temperature gradient calculated from the heat balance.

In the model presented in this paper the discretised form of equation (20), equation (21) is used because of the availability of calculated temperature points relating instantaneous thermal gradients through a test laminate at various stages of decomposition and combustion. Thus using the temperature data, together with β, the mass transfer coefficient the volatile mass transfer rate can be calculated.

$$\dot{m}_{vol,i}(x,t) = -\beta_T \rho_i (1 - f_{char,i}) \left[\frac{T_{i-1} - T_i}{(x_{i-1} + x_i)/2} \right] \tag{21}$$

The mass balance of the i-1th layer is updated by adding the value of $m_{vol}(x,t)$ to the concentration of volatiles already within the ith layer, $C_{vol,i-1}$ i.e. $C_{vol,i-1} = C_{vol,i-1} + m_{vol,i}(x,t)$. A value of $\beta_T = 3.788 \times 10^{-10}$ m^2 s^{-1} K^{-1} was used satisfactorily within a credible mass transport model developed by Staggs, [18], and has been adapted in our model as a first approximation. However it remains to establish an accurate experimental value of this parameter for the polymeric system of interest in this study i.e. a 50:50 w/w mixture of epoxy resin and woven E-glass.

5.2 Results and Validation of Model C

The results of the modified heat transfer model, (Model C) are shown in Figures 2(c), 3(c), 4(c) and 5(c). Surprisingly, examination of Figures 2(c) and 3(c) show that the activation of a mass transfer module within the heat transfer model has practically no effect on either the temperature or mass output. In contrast to the incorporation of temperature-variable physical properties, the mass transfer phenomenon as modelled does not improve the fit of either the temperature or mass loss curves generated. This shows that the instantaneous proportion of volatiles transferred out of each calculation layer is insignificant when compared to the amount generated by decomposition within each layer.

6 Model D: Heat Transfer Model With Ignition

Here, we discuss the addition of new calculation routines in the above model, which are intended to predict and calculate the onset of both volatile ignition and solid-phase combustion, and the heat of combustion generated during both phenomena.

6.1 Theory of Flaming Combustion

The prediction of combustion from first principles is a task which requires the use of fundamental thermodynamics. Equations have been outlined by Kanury, [21], via an application of the 1st law of thermodynamics describing energy conservation, which govern the onset of the combustion process. They are written by considering idealised adiabatic and isothermal combustion scenarios. Using these, two principal idealised energy balances may be written for a system, one for a perfectly isothermal system, the second for the perfectly adiabatic system as given by Eqns. 22 and 23 respectively, [21]:

$$V\dot{Q}_{comb} - hA_{surf}\left(T_s - T_h\right) = 0 \tag{22}$$

$$V\dot{Q}_{comb} - \rho c_p V \frac{dT}{dt} = 0 \tag{23}$$

In both these expressions, the first common term represents the heat generated by the exothermic combustion reaction, where V is the total volume of the combusting gas and Q is its heat of combustion. In Equation 22 for the isothermal case, the second term represents all of that heat being withdrawn from the system through the surface area, A_{surf}. This generally occurs by means of a combination of convection and radiation, where the system at temperature T_s is surrounded by an external fluid at temperature T_h. In Equation 23, for the adiabatic case, the second term is different and is now a measure of the trapped heat absorbed by the gas as the combustion progresses. Since all of the heat generated by combustion is retained in the system, there must be an increase in temperature with time.

However, real combustion processes may be represented as a hybrid of these two cases resulting in a combined system energy balance which may be written as a combination of Eqns. 22 and 23, (Eqn. 24).

$$V\dot{Q}_{comb} - \left[\rho c_p V \frac{dT}{dt} - hA_{surf}\left(T_s - T_h\right) \right] = 0 \tag{24}$$

This equation forms the basis for developing mathematical criteria for spontaneous ignition. These criteria normally include critical spontaneous ignition temperature and time, as well as critical heat and gas mass fluxes. The first basic condition which must be satisfied is derived from (24) and is given by (25), [21], and is the *criterion of positive heat balance* for spontaneous ignition.

$$\Delta h_{comb} V \dot{m}_{vol} \geq hA_{surf}\left(T_s - T_h\right) \tag{25}$$

Here, m_g is the mass of gas. It is written with the assumption that near the spontaneous ignition point, the system may be assumed to approach adiabatic conditions, because the rate of heat generation is far greater than the corresponding rate of heat transfer across the system boundary.

The rate of gas combustion may be represented by a kinetic expression of the form of (26), [21], where either a combined concentration-and-temperature power law or an Arrhenius expression may be used.

$$\frac{d\dot{m}_{vol}}{dt} = k'_n C_{vol}^{n'} T^m = k_n C_{vol}^n \exp\left(-E_{comb}/RT\right) \tag{26}$$

(26) is now substituted into the adiabatic energy balance expression, (25), and the result is integrated resulting in an expression for the temperature profile of a pseudo-adiabatic combustion system, (27);

$$\left(\frac{T}{T_0}\right)^{m-1} = \left[1 - \frac{t}{\left(\frac{\rho c_p T_0}{(m-1)\Delta h_{comb} k'_n C_{vol,0}^{n'} T_0^m} \right)} \right]^{-1} \tag{27}$$

This allows a definition to be written for a critical time-point t_{ign}, which represents the instant of ignition and may be regarded as the spontaneous ignition time, (28), [21];

$$t_{ign} \equiv \frac{\rho c_p T_0}{(m-1)\Delta h_{comb} k'_n C_{vol,0}^{n'} T_0^m} \tag{28}$$

If an Arrhenius type expression is used instead to express the rate of gas consumption during combustion, (28) may take the alternative format, (29), [21];

$$t_{ign} \equiv \rho c_p . \frac{RT_0^2}{E} . \frac{\exp(E_a / RT_0)}{\Delta h_{comb} k_n C_{vol,0}^n} \tag{29}$$

Here, t_{ign} is the time of ignition or the ignition delay time, ρ is the material density, c_p its specific heat capacity, R, the real gas constant, T_0 the initial temperature of the material, E_a the activation energy of the combustion reaction, Δh_{comb} the heat of combustion, k_n the rate constant of the reaction, $C_{vol,0}$, is the initial concentration of combusting material and n is the order of the combustion reaction

Using similar thermodynamic derivations, the instantaneous critical heat density, Q_{comb}, [J m^{-3}], at the lower flame limit for the combustion process is defined by Eqn. (30), at the flame temperature of the combustion, T_f, Lyon et. al., [5].

$$Q_{comb} = \frac{\rho c_p (T_f - T_h)}{(1-\chi)} \tag{30}$$

Here, ρ is the density of the laminate, T_f and T_h are the flame and headspace temperatures respectively, c_p is the specific heat capacity of the laminate and χ is the efficiency of the combustion reaction

The corresponding critical volatile mass flux, defined as the lowest volatile flux necessary to sustain combustion at a given temperature, is given by Eqn. (31), [5];

$$\dot{m}_{vol,LFL} = \frac{hQ_{comb}}{\rho c_p \Delta h_{comb}} \left(1 - \left[\frac{T_{ign} - T_0}{T_f - T_0} \right] \right) \tag{31}$$

The critical temperature that must be reached for ignition to take place is called the ignition temperature, T_{ign} and is given by Eqn (32), [5]

$$T_{ign} = \left[\frac{T_0 h_g}{c_p} \right]^{0.5} \quad (32)$$

Thus, for the case of a solid at 298 K, with a specific heat capacity of 1540 J kg^{-1} K^{-1}, (Table 1), and a heat of gasification of the order of 2 MJ kg^{-1}, the calculated ignition temperature is 622 K, (349°C). This value can now be used to calculate the critical heat density and volatile mass flux respectively, from Eqns. (30) and (31), which are 1.87 x 10^4 W m^{-2} and 0.28 mol m^{-2} s^{-1} respectively. This latter value would equate to a critical methane flux of 4 g m^{-2} s^{-1} for the physical properties and combustion conditions described in Table 1. In the present model, it was decided to employ Eqns. (30), (31) and (32) as the three minimum conditions necessary for combustion to occur. Upon all three conditions being satisfied by the instantaneous temperature, surface heat flux and surface volatiles flux respectively, the additional heat term, $Q_{comb,i}$ was activated within the finite difference equations for temperature increment as given by Eqns. 5-7. Where this "triple condition" was not satisfied, the $Q_{comb,i}$ term was switched to zero.

6.2 Results and Validation of Model D; Heat Transfer Model With Ignition and Combustion

The ignition and combustion model, (Model D), was tested by the use of existing temperature and mass loss data for two specimens of epoxy based composites results for EP are shown in Figures 2(d) and 3(d) and for EP20 in Figures 4(d) and 5(d). Qualitatively, examining temperature data and model for the control sample, EP in Figure 2(d), it can be seen that the experimental and simulated temperature curves are broadly in agreement, with the simulated data anticipating the surface temperature rise with an almost identical curvature, although it systematically overestimates the measured surface temperature by 10 – 15 K. There may be a number of reasons for this, such as :

1. Low convective heat transfer coefficient value used in the model,
2. *Low radiative reflectivity in the model:*
3. *Low thermal conductivity value in the model: Low specific heat capacity in the model***:**

4. *Low experimental surface temperature measurement:*

Comparing the scenarios 1 – 4, in the initial heat-up phase, it would appear that while each is possible, and while a combination of all of these factors might be at work together in the present case, the more likely modelling error scenarios are those of a low value of specific heat capacity in the model, (with perhaps a low thermal conductivity). These scenarios would not be affected by the eventual convergence of simulated and measured temperatures observed after t = 200 s, since decreasing temperature gradient would reduce the effect of an inaccurate thermal conductivity value and, secondly, since the solid would be almost heat saturated under such a temperature convergence, with an insulated bottom surface, meaning that the distorting effect of an inaccurate specific heat capacity within the simulation would be reduced. Hence, scenarios 3 and 4 seem feasible explanations for the observed discrepancies for all of these reasons.

Examining possible errors in the experimental method, (Scenario 5), it is equally likely that the thermocouple on the surface was insufficiently attached to the top surface of the laminate, so that it was either completely or partially measuring the atmospheric temperature rather than the solid surface temperature. This explanation would sufficiently explain the substantial qualitative discrepancy between simulated and measured upper temperature during the actual flaming combustion event in the headspace over the laminate from $74 < t < 200$ s.

Examination of the middle temperature curves of the two composites, EP and EP20, both experimental and simulated for Model D from Fig. 2(d) and Figure 4(d) shows some interesting trends. For EP, (Fig. 2d), it can be seen that the simulated middle temperature curve tracks the *bottom* rather than the middle temperature data almost completely during the first 100 s, before deviating considerably from the data after this point. On the basis of this difference, it is probable that the simulated thermal capacity of the EP composite is far greater than is actually the case, resulting in lower predicted values for both middle

and bottom temperatures, something which is primarily explicable in terms of excessively high specific heat capacity and low thermal conductivity in the model.

However, in the equivalent heating phase of the EP20 composite all three simulated and experimental temperature curve-pairs are in good qualitative agreement; at least until the top temperature curves diverge suddenly at 67 s, followed by a delayed divergence of the simulated and actual middle temperature curves at 100 s. Despite this, it will be noticed that the experimental data for the middle laminate temperature clearly indicates that the actual middle temperature being achieved is higher than the recorded temperature of the surface thermocouple from approximately 197 s by an average of 10 - 15°C. This may be explained by the fact that by 197 s, much of the resin above the middle layer thermocouple has been burnt away, effectively creating a new surface layer in the region of the original composite middle layer, i.e. the middle thermocouple is now the 'top' thermocouple.

Examining Figure 3(d) and 5(d) which show the mass loss curves for the same EP and EP20 studies, it can be seen that there is better qualitative agreement between simulated and experimental mass curves in both cases than is achieved by any of the previous models A – C, though there is still the same tendency to systematically underestimate mass loss in both cases to a certain time-point, after which the model overestimates the rate of mass loss. In the case of EP this point of transition is 65 s, for EP20 it is 238 s. After both points, theoretical mass loss continues until a finite minimum residual mass determined by the char selectivity, a parameter of the program, is reached. These yields are 6 and 20% respectively for EP and EP20, meaning that residual masses of 53 and 60% are the minimum possible outputs of the model, which also accounts for the presence of 50% glass in these values. In the present case, the remarkable feature of the model curves for both materials is the fact that the experimental retained mass data agrees so closely with the final theoretical residual mass. For EP, the actual residual mass achieved is 55.6%, just fractionally above the 55.4% predicted by the model, and 2.4% above the minimum threshold for EP,

indicating the formation of char. For EP20, actual residual mass is 63.2%, which is only slightly in excess of the predicted value of 63.4%. Here again, both experiment and model agree on the formation of just in excess of 3.4% residual organic char, 1% more than that of EP.

Overall, the deviation in the experimental and predicted mass loss curves could be explained in a number of ways: firstly it is important to remember that the curvature of both mass loss data curves in both cases shows abrupt discontinuity after approximately 40 and 30 s respectively for EP and EP20, indicating a near step-change in conditions which is not being predicted by the model. One explanation for this could be the use of an insufficiently high rate constant of decomposition for the epoxy resin, but this would not produce the 'kinked' curvature required to accurately model the real mass loss data. Other factors could have been specific environmental conditions of the cone test on the day; although the fact that both EP and EP20 display this step-phenomenon in common would discount the probability of an artefact in the measurement, unless it was systematically common to both experiments.

6.2 Prediction of time-to-ignition

A theoretical thermodynamic expression, for the prediction of composite ignition time was developed from thermodynamic principles by Kanury, [21], (Eqn. 31) as discussed in Section 6.1 Implementing this equation for a typical combustion of pure methane for example, and substituting parameters given in Table 1, we arrive at a curve for ignition delay time which is a function of the starting temperature of a laminate at the instant when an external heat flux Q_{ext} is activated; Figure 9.

Clearly, it can be seen from Figure 9 that the magnitude of ignition delay time is significantly reduced with increase of the laminate starting temperature, T_0, from a value of 57 s at 25°C to only a few seconds at a temperature of 377°C. This latter figure for ignition temperature compares moderately well with the value actually observed for the EP composite plaque which was 400°C at an ignition time of approximately 74 s, and even better with the equivalent ignition point for EP20, (360°C at 65 s). However, it underestimates

the actual ignition *time delay* of EP and EP20 respectively by 17 and 8 s. Thus the model which in its current form is designed to predict ignition time is actually better at indirectly predicting ignition temperature. The most likely reason for this premature prediction of ignition is probably the absence of any terms in this stand-alone expression to account for heat loss, which would explain the further delay in ignition actually observed. Such an adjustment would most probably result in the curve of Figure 9 being shifted to the right along the time axis, without substantial alteration of its curvature. It will also be remembered that the curve is calculated for the combustion of pure methane, and is thus not truly representative of the actual activation energy of combustion which would be required for the actual volatile mixture evolved.

Clearly, a stand-alone calculation such as Eqn. 31 helps to establish the important points in the combustion cycle and to create representative expressions in an overall model for the critical ignition and combustion criteria, although it can never completely replace experimental observation of ignition point as the definitive indicator, because of the influence of local conditions such as heat loss and convection on ignition in practice.

7.0 Conclusions

In the present paper a model based on the well-known Henderson's heat transfer equation has been used to predict the temperature through the thickness of the control and flame retarded composite samples. The model has been altered to allow ignition and combustion phenomena of structural composite materials to be predicted and quantified from first principles using known physical and thermodynamic data for the included resins and additives. This modification has consisted of two principal components; 1) a mathematical mechanism for recognition of the correct temperature of ignition, and 2) a calculation of the correct heat of combustion generated during the exposure time of interest. This has allowed a model of good qualitative character to be achieved, which is generally faithful to mass and temperature

data obtained by cone calorimeter for these composite laminates. However, there are still some points of departure between the model and this data.

Thus, there remains the challenge of improving the quantitative fit of the model by implementing the following measures:

1. Improving the quality of *in-situ* temperature data obtained at the surfaces of burning composites, preferably by means of non-contact methods which are not vulnerable to detachment because of receding resin. Such methods would also exclude the possibility of recording volatile phase temperatures rather than true surface temperature as relevant to the model in its current form.
2. Further enhancing the quality of physical property data deployed. In particular, determining a truly accurate temperature sensitivity of physical properties, and correctly representing the overall physical properties of a composite in terms of the individual physical properties of the components.
3. Full identification and quantitative profiling of the individual volatile species released during decomposition of a composite material, obtained by quantitative volatile analysis using gas chromatography.
4. Obtaining more accurate volatile diffusivity / permeability parameters through decomposing structural composites and char networks. The acquisition of such data ideally requires permeation testing of the composite material during combustion.

It is anticipated that implementation of some or all of these measures would result in a model of true quantitative fidelity to cone calorimetry data, which could ultimately be used as a partial substitute for experiment in the early stages of composite formulation and fire testing. In terms of predicting burning behaviour, volatile mass loss rates and heat release rates can help to identify different burning phases, during the combustion of a composite panel which appear as separate peaks in each curve. The shape of temperature profile curves can indicate how gradual or abrupt burning behaviour is, while the difference between surface and base temperatures can predict speed of like burn-through.

Nomenclature

Symbol	Variable	Unit
A_{surf}	Surface area of laminate	m^2
α	Instantaneous fraction of resin and fibre in layer i	-
α	Thermal diffusivity of laminate	$W\ m^{-2}\ K^{-1}$
β	Permeability of solid composite to volatiles	m^2
β_T	Thermal volatiles diffusivity coefficient	$m^2\ s^{-1}\ K^{-1}$
C_g	Concentration of volatiles in Eqn. 31	$mol\ m^{-3}$
E_a	Activation Energy	$J\ mol^{-1}$
Fo	Fourier Number	-
f_{resin}	Instantaneous fraction of resin in composite slab	-
f_{char}	Instantaneous fraction of char in composite slab	-
f_{vol}	Instantaneous fraction of volatiles in composite slab	-
f_{solid}	Instantaneous fraction of solid in composite slab	-
H	Instantaneous enthalpy of system	$J\ mol^{-1}$
ΔH	Enthalpy of Combustion, (Eqn. 31)	$J\ mol^{-1}$
Δh_{comb}	Enthalpy of combustion, (Eqn. 34)	$J\ mol^{-1}$
h_g	Heat of volatilisation	$J\ mol^{-1}$
m	Index in kinetic expression of Eqn. 31	-
P	Pressure of system	Pa
Q_{net}	Net Heat Flux absorbed at surface	$W\ m^{-2}$
Q_{ext}	Total external heat flux incident to surface	$W\ m^{-2}$
Q_i	Total heat flow in i^{th} layer	$W\ m^{-2}$
Q_n	Total heat flow in the bottom n^{th} layer	$W\ m^{-2}$
$Q_{comb,i}$	Total heat of combustion in i^{th} layer	$W\ m^{-2}$
$Q_{decomp,i}$	Total heat of decomposition in i^{th} layer	$W\ m^{-2}$

T_s	Surface temperature	K
T_f	Flame temperature	K
T_h	Headspace air temperature (above surface)	K
T_i	Temperature of the i^{th} layer in the solid	K
T_{ign}	Ignition temperature	K
ε	Radiative emissivity of top surface	-
σ	Stefan-Boltzmann constant = 5.68×10^{-8}	$J\ K^{-4}$
k	Thermal conductivity	$W\ m^{-1}\ K^{-1}$
k_{pyr}	Reaction rate constant of decomposition	s^{-1}
m_{vol}	Mass flowrate of volatiles leaving solid	$kg\ m^{-2}\ s^{-1}$
h_{conv}	Convective heat transfer coefficient	$W\ m^{-2}\ K^{-1}$
h_{vol}	Enthalpy of volatiles	$J\ kg^{-1}$
h_{char}	Enthalpy of char, (partially decomposed resin)	$J\ kg^{-1}$
μ	Dynamic viscosity of the solid composite	$N\ m^{-2}\ s$
ρ	Density of the resin	$kg\ m^{-3}$
c_p	Specific heat capacity	$J\ kg^{-1}\ K^{-1}$
x_i	Instantaneous thickness of calculation layer i	m
$x_{i,decomp}$	Layer thickness for decomposition only	m
$x_{i,comb}$	Layer thickness for combustion only	m
s_{char}	Selectivity of decomposition reaction for char	-
s_{vol}	Selectivity of decomposition reaction for volatiles	-
t	Time interval of simulation	s
v_0	Superficial velocity of volatiles through the laminate	$m\ s^{-1}$
w	Number of mass or mole units of resin	kg or mole
w_{char}	Number of mass or mole units of char	kg or mole
w_{vol}	Number of mass or mole units of volatile species	kg or mole

References

1. Henderson J.B., Wiebelt J.A., Tant M.R., *J. Compos. Mater.* **19**, (1985), p. 579
2. Gibson A.G., Mouritz A.P., 'Fire Properties Of Polymer Composites' in 'Solid Mechanics And Its Applications' Ed. Gladwell G.M.L., (2006), Springer, **143**, p. 140-168,
3. Drysdale D., Grant G., 'Numerical modelling of early flame spread in warehouse fires', *Fire Safety Journal* **14***,* (1995), p. 247
4. Drysdale D., Kuang-Chu**ng,** T., 'Using cone calorimeter data for the prediction of fire hazard', Fire Safety Journal **37,** (2002), *p. 697*
5. *Lyon R.E, Qu***in***ti*ere J.G., 'Criteria for piloted ignition of combustible solids', *Combustion and Flame* **151**, (2007), p. 551
6. Lyon R.E., 'Decomposition kinetics of char-forming polymers', *Polymer Degradation and Stability* **61, (**1998), p. 201
7. Staggs J.E.J., Whiteley R.H., 'Modelling the combustion of solid-phase fuels in cone calorimeter experiments', *Fire Mater*. **23**, (1999), p. 63
8. Staggs J.E.J., 'Ignition of char-forming polymers at a critical heat flux', *Polymer Degradation and Stability,* **74**, (2001), p. 433
9. Staggs J.E.J, Watt S.D., McIntosh A.C., Brindley J., 'A theoretical explanation of the influence of char formation on the ignition of polymers', *Fire Safety Journal,* **26**, (2001), p. 421
10. Staggs J.E.J., 'A simple model of polymer decomposition including mass transport of volatiles', *Fire Safety Journal,* **34,** (2000), p. 69
11. Staggs J.E.J., 'Modelling thermal degradation of polymers using first-order kinetics', *Fire Safety Journal* 32, (1999) p. 17
12. Galgano A., Di Blasi C., Branca C., Milella E., 'Thermal response to fire of a fibre-reinforced sandwich panel: Model formulation, selection of intrinsic properties and experimental validation' *Polymer Degradation and Stability,* **94**, (2009), p. 1267
13. Kandare E., Kandola B.K., McCarthy E.D., Myler P., Edwards G., Jifeng Y., Wang Y.C.,' Fibre-reinforced epoxy composites exposed to high temperature environments. Part II: Modelling mechanical property degradation', J Composite Materials, Published online in advance of print: November 10, 2010, doi: 10.1177/0021998310385024.
14. Kandare E., Kandola B.K., McCarthy E., Myler P., Edwards G., Jifeng Y., Wang Y.C., 'Fibre-reinforced epoxy composites exposed to high temperature environments. Part I: Experimental data acquisition, Published online before print September 3, 2010, doi: 10.1177/0021998310373511.
15. Neininger S., Staggs J.E.J., Horrocks R.E., Hill N.J., 'A study of the global kinetics of thermal degradation of a fibre-intumescent mixture', *Polymer Degradation and Stability* **77** (2002) p. 187

16. Kandare E., Kandola B.K., Staggs J.E.J., 'Global kinetics of flame retarded epoxy resin formulations', *Polymer Degradation and Stability* **92** (2007) p. 1778
17. Incropera F. P., DeWitt D. P., 'Fundamentals of Heat and Mass Transfer', 5th ed., Wiley.
18. Staggs J.E.J., 'Heat and mass transport in developing chars', Polymer Degradation and Stability **82** (2003) p. 297
19. Neĭman M. B., Kovarskaya B. M., Golubenkova L. I., Strizhkova A. S., Levantovskaya I. I., Akutin M. S., 'The thermal degradation of some epoxy resins', J. Polym.Sci. 56, (1962), 164, p. 383–389
20. Perry R.H., Green D.W., Maloney J.O. eds. 'Perry's Chemical Engineer's Handbook', 1999, 7th Edition, Chapter 2, p. 2-144
21. Kanury A.M. 'Introduction to Combustion Phenomena' from 'Combustion Science and Technology Book Series', Ed. Glassman, I., Gordon & Breach, London, 1975, ISBN 067702690
22. Perry R.H., Green D.W., Maloney J.O. eds. 'Perry's Chemical Engineer's Handbook', 1999, 7th Edition, Chapter 5, p. 5-15
23. Tsilingiris P.T., Energy Convers. Manage. 44 (2003) 2839–2856.
24. Stoliarov S.I., Crowley S., Lyon R.E., Linteris G.T., 'Prediction of the burning rates of non-charring polymers', Combustion and Flame, 156, (2009), 1068–1083
25. Lautenberger C. et. al., 'Gpyro' combustion code, online at URL; http://code.google.com/p/gpyro.
26. Lautenberger C., Zhou, Y.Y. and Fernandez-Pello, A.C., "Numerical Modeling of Convective Effects on Piloted Ignition of Composite Materials", *Combustion Science and Technology,* **177** 1231-1252 (2005).
27. Lautenberger, C., Kim, E., Dembsey, N. & Fernandez-Pello, C., "The Role of Decomposition Kinetics in Decomposition Modeling – Application to a Fire Retardant Polyester Composite," *Fire Safety Science* 9: 1201-1212 (2008). http://me.berkeley.edu/cpl/publications/9th_iafss_paper_149.pdf

Table 1. Physical Properties and Reaction Parameters of Decomposition and Combustion for EP and EP20 composites as used in Predictive Combustion Model

Properties	**Units**	**Resin Formulation Property Values**			
		EP Control Resin		**EP20 Fire Retardant Resin**	
		Resin-Fibre	**Char-Fibre**	**Resin-Fibre**	**Char-Fibre**
s_{char}		0	0.53	0	0.6
k	W m^{-1} K^{-1}	0.162	0.1	0.182	0.1
c	J kg^{-1} K^{-1}	1540	1000	1686	1000
ρ	kg m^{-3}	1500	1047	1444	1047
A_{PYR}	s^{-1}	2.16E+06	2.16E+06	1.99E+03	1.99E+03
E_{PYR}	J mol^{-1}	1.17E+05	1.17E+05	6.50E+04	6.50E+04
H_{PYR}	J kg^{-1}	-1.98E+05	-1.98E+05	-2.95E+05	-2.95E+05
A_{COMB}	s^{-1}	2.00E+08	2.00E+08	2.00E+08	2.00E+08
E_{COMB}	J mol^{-1}	1.00E+05	1.00E+05	1.00E+05	1.00E+05
H_{COMB}	J mol^{-1}	2.00E+06	2.00E+06	2.00E+06	2.00E+06
b	m^2 s^{-1} K^{-1}	1.00E-12	1.00E-12	1.00E-12	1.00E-12
C_g^0	mol m^{-3}	84			

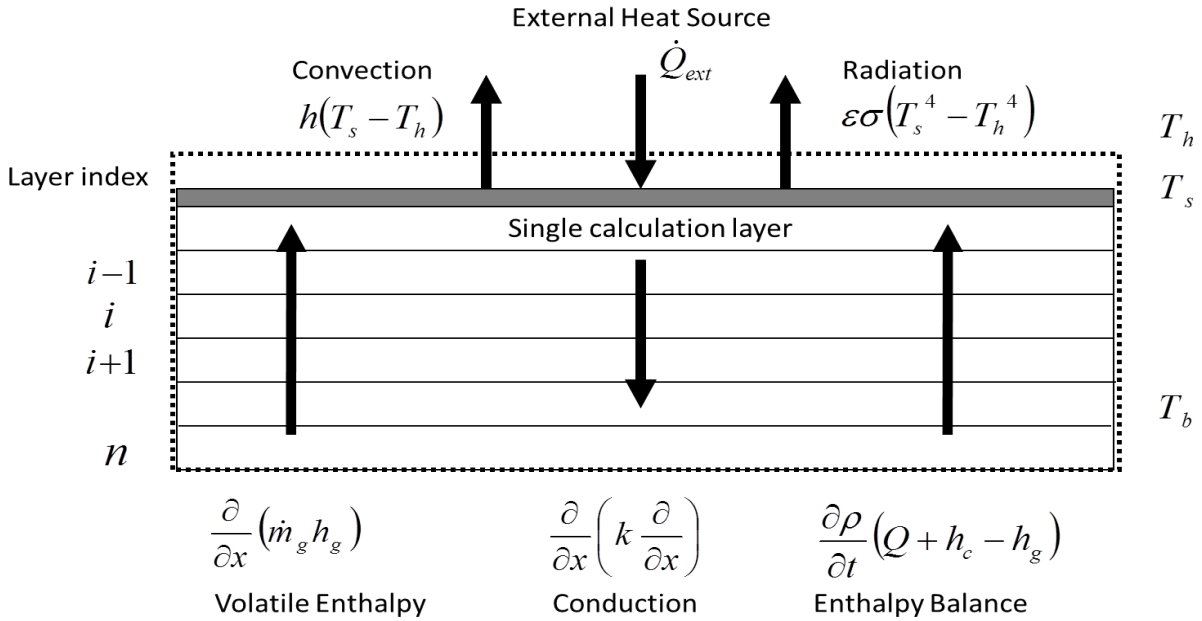

Figure 1. Schematic representation of a structural laminate exposed to a steady-state external heat flux from an overhead source, and the movements of heat associated with the system.

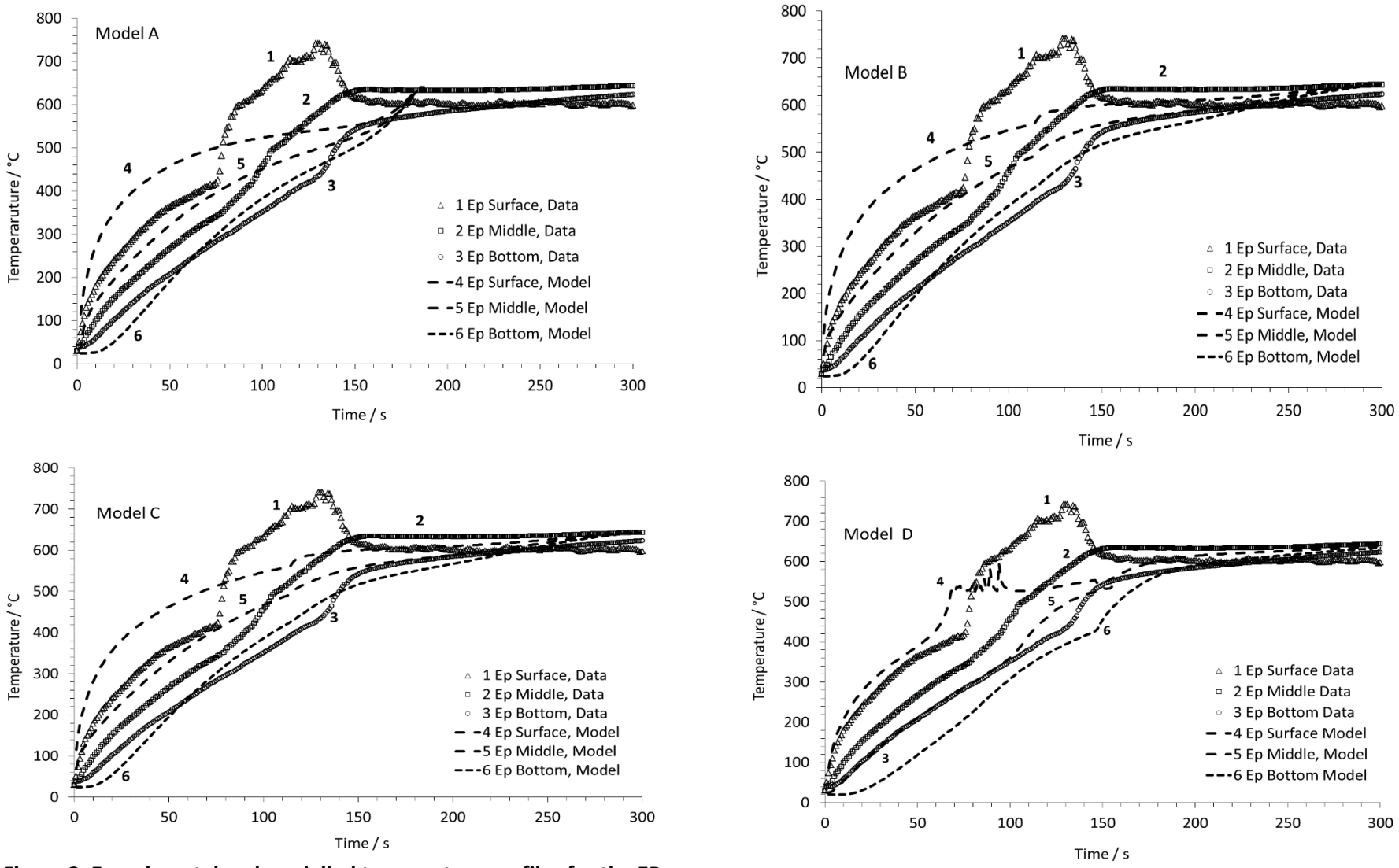

Figure 2. Experimental and modelled temperature profiles for the EP composite exposed to one-sided heat flux of 50 kW / m^2: a) Model A, b) Model B: with temperature-dependent physical properties, c) Model C: A + B + mass transfer and d), Model D: A + B + C + ignition/combustion

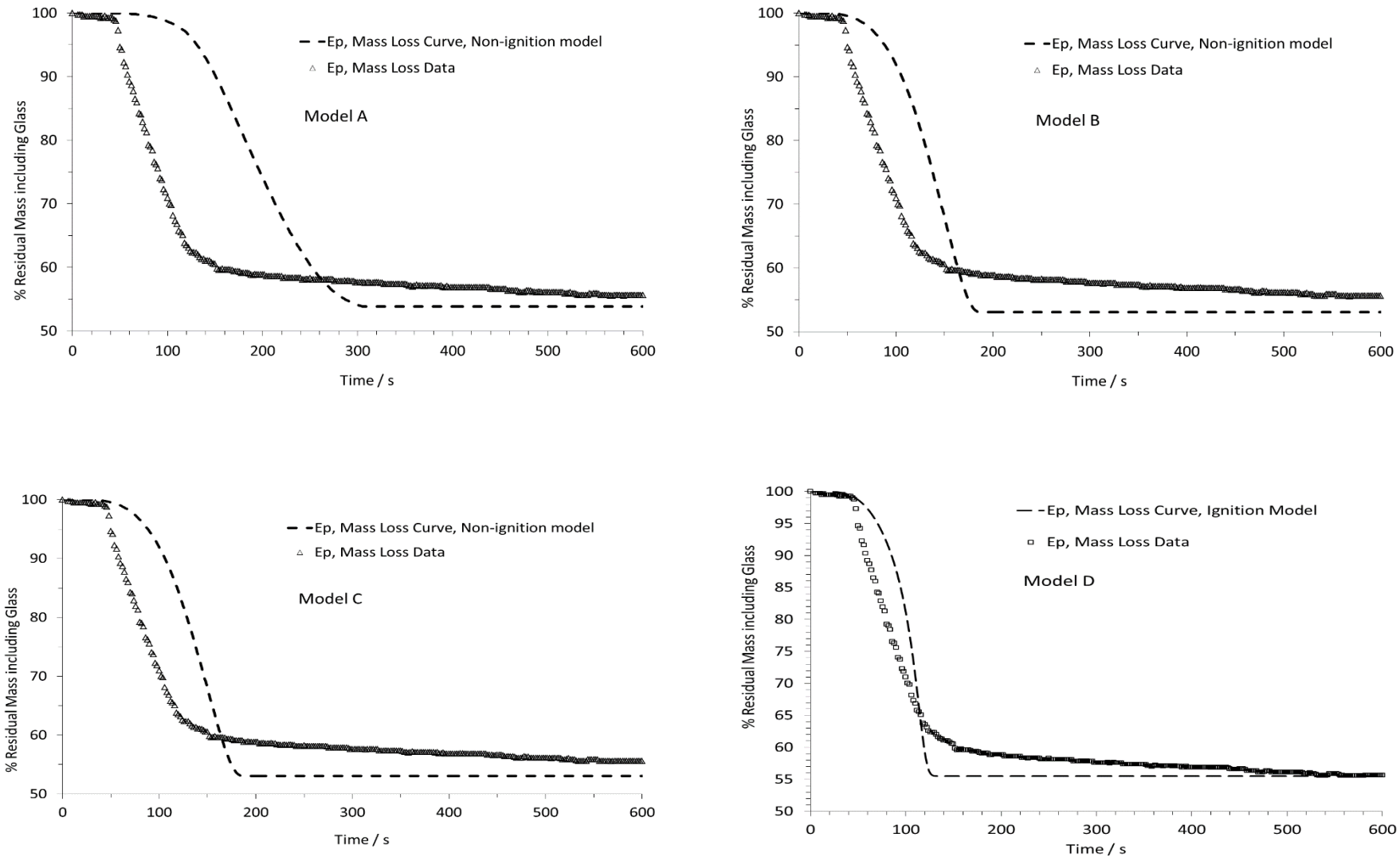

Figure 3. Experimental and modelled mass loss profiles for the EP composite exposed to one-sided heat flux of 50 kW / m^2 : a) Model A,b) Model B with temperature-dependent physical properties, c) Model C: A + B + mass transfer and d) Model D: A + B + C + ignition/combustion.

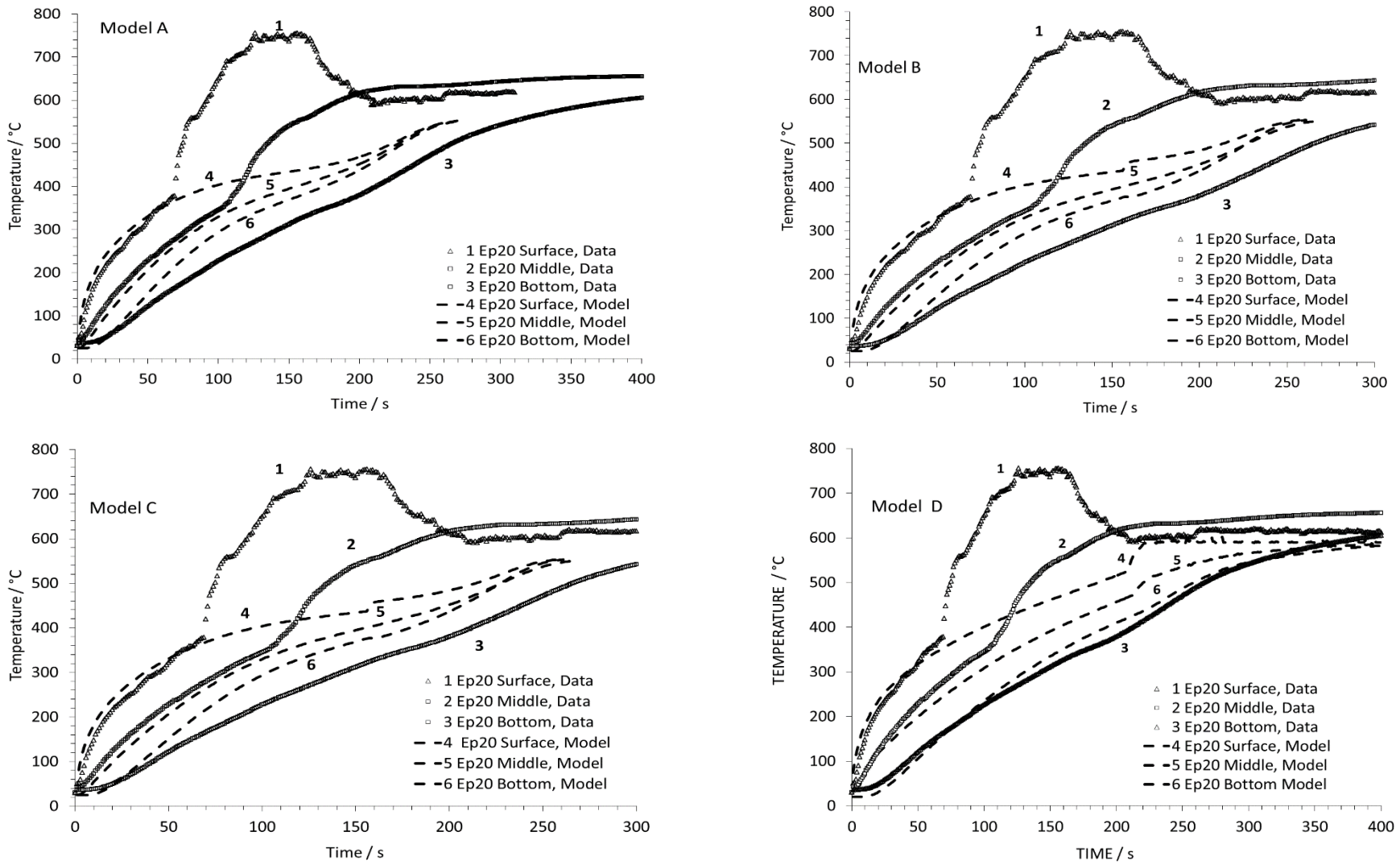

Figure 4. Experimental and modelled temperature profiles for the EP20 composite exposed to one-sided heat flux of 50 kW / m^2 : a) Model A, b) Model B: with temperature-dependent physical properties, c) Model C: A + B + mass transfer and d) Model D: A + B + C + ignition/combustion

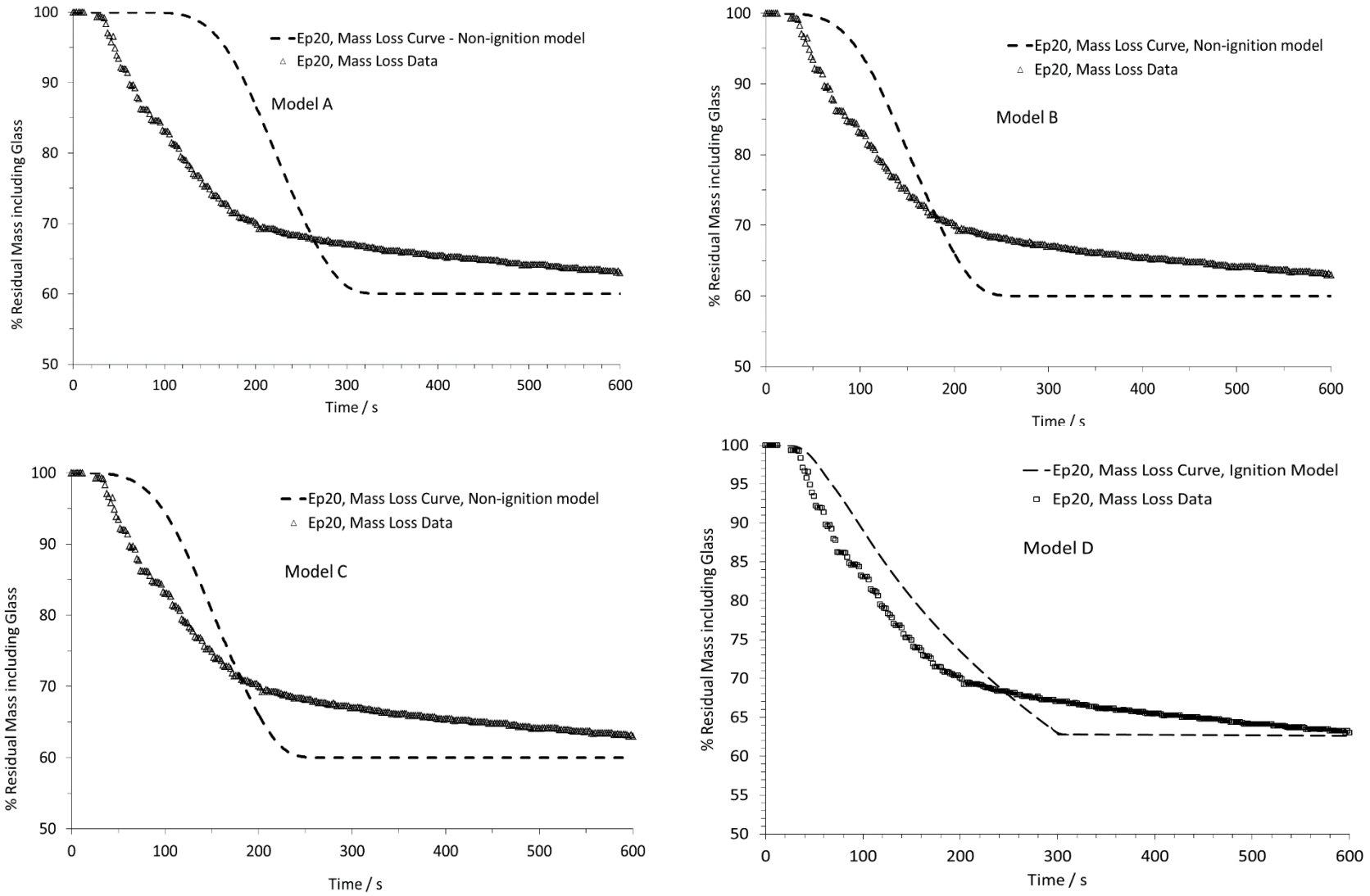

Figure 5. Experimental and modelled mass loss profiles for the EP20 composite exposed to one-sided heat flux of 50 kW / m^2 : a) Model A,b) Model B with temperature-dependent physical properties, c) Model C: A + B + mass transfer and d) Model D: A + B + C + ignition/combustion.

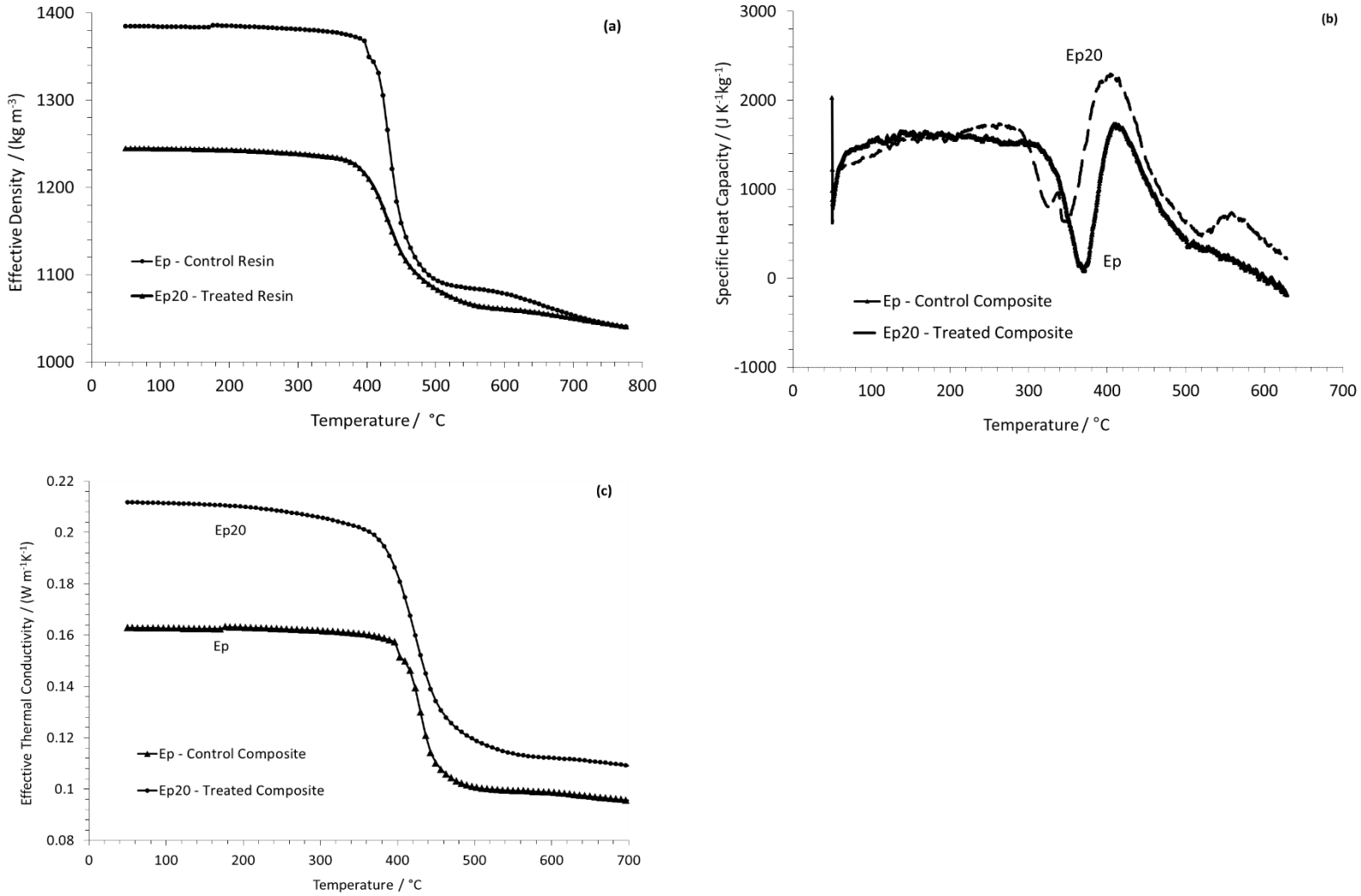

Figure 6. Temperature dependent a) Effective overall density, b) effective specific heat capacity and c) effective thermal conductivity for EP and EP20 composites

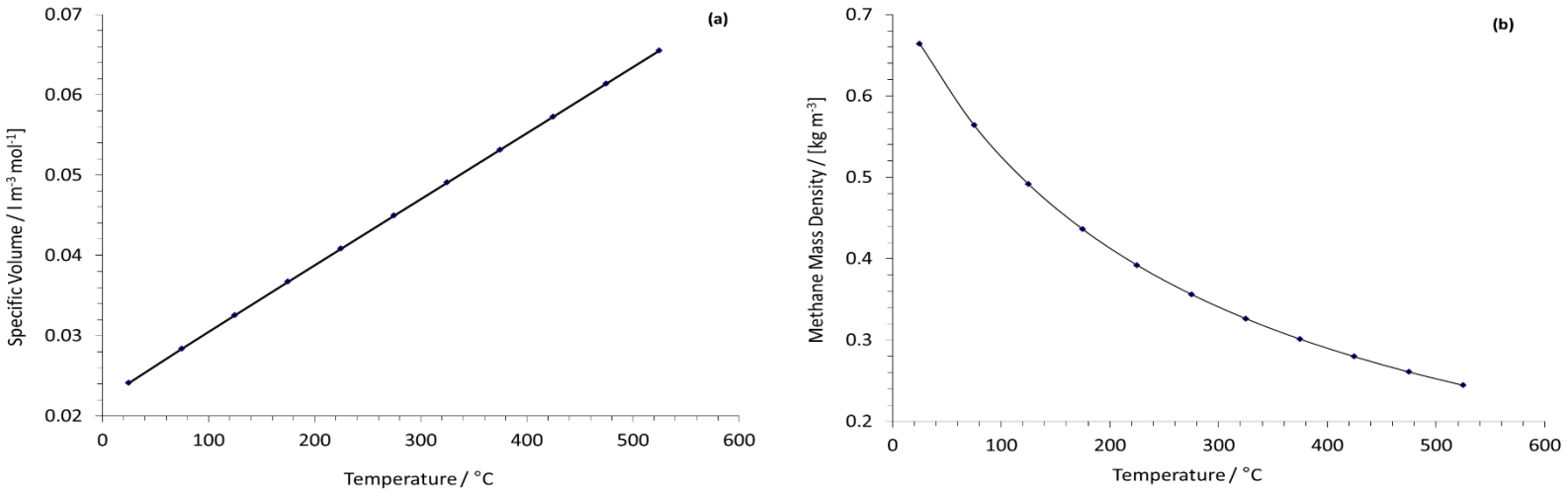

Figure 7. Temperature dependency of methane (a) molar volume and (b) specific density.

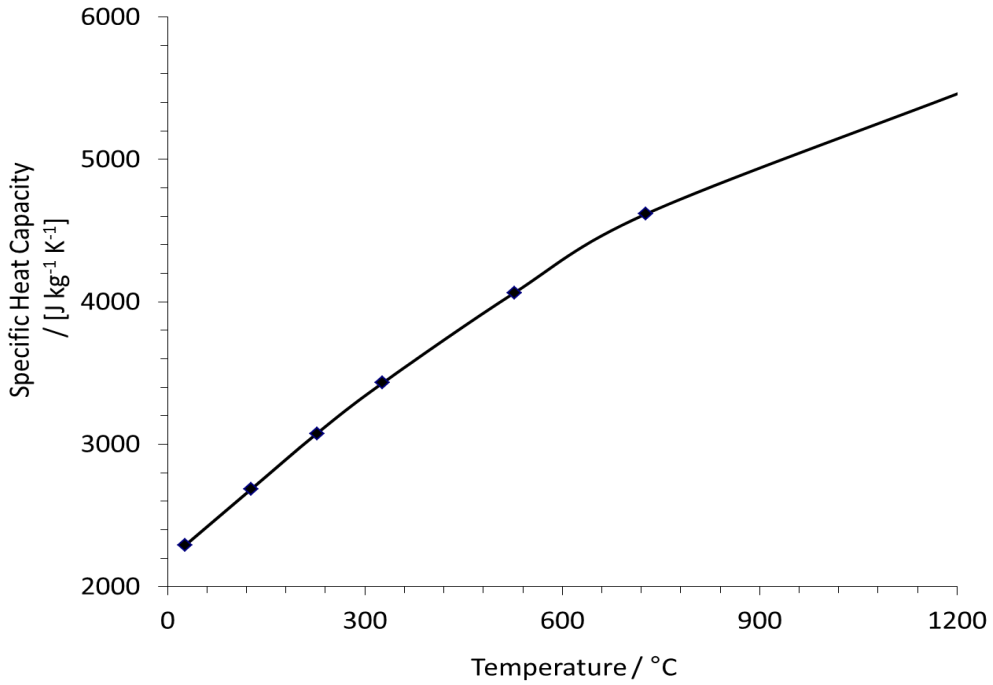

Figure 8. Specific heat capacity of methane with temperature; Atom Contribution Method

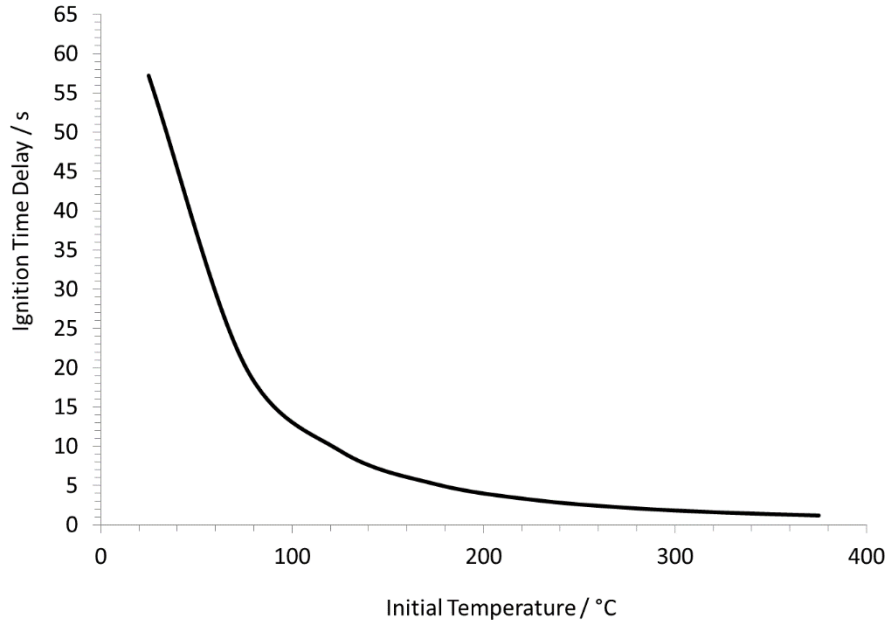

Figure 9. Ignition time delay from a reference temperature of 25°C as calculated using Eqn. 35 for a typical resin system at initial temperature of 298K